Differential proteomic profiling of primary and recurrent chordomas

SU CHEN[1*], WEI XU[1*], JIAN JIAO[1], DONGJIE JIANG[1], JIAN LIU[2], TENGHUI CHEN[3], ZONGMIAO WAN[1], LEQIN XU[1], ZHENHUA ZHOU[1] and JIANRU XIAO[1]

[1]Department of Bone Tumor Surgery, Changzheng Hospital, Second Military Medical University, Shanghai 200003, P.R. China; [2]Department of Molecular and Cellular Biology, Baylor College of Medicine; [3]Department of Bioinformatics and Computational Biology, The University of Texas M.D. Anderson Cancer Center, Houston, TX 77030, USA

Received October 12, 2014; Accepted December 19, 2014

DOI: 10.3892/or.2015.3818

Abstract. Chordomas are locally destructive tumors with high rates of recurrence and a poor prognosis. The mechanisms involved in chordoma recurrence remain largely unknown. In the present study, we examined the proteomic profile of a chordoma primary tumor (CSO) and a recurrent tumor (CSR) through mass spectrum in a chordoma patient who underwent surgery. Bioinformatic analysis of the profile showed that 359 proteins had a significant expression difference and 21 pathways had a striking alteration between the CSO and the CSR. The CSR showed a significant increase in carbohydrate metabolism. Immunohistochemistry (IHC) confirmed that the cancer stem cell marker activated leukocyte cell adhesion molecule (ALCAM or CD166) expression level was higher in the recurrent than that in the primary tumor. The present study analyzed the proteomic profile change between CSO and CSR and identified a new biomarker ALCAM in recurrent chordomas. This finding sheds light on unraveling the pathophysiology of chordoma recurrence and on exploring more effective prognostic biomarkers and targeted therapies against this devastating disease.

Introduction

Chordoma is a rare slow-growing neoplasm thought to arise from cellular remnants of the notochord. The incidence of chordoma is approximately 1 case in one million individuals and it accounts for ~1-4% of all tumor cases. However, these rare tumors present very significant treatment challenges (1). It is notable that 67% of the surgically managed patients suffer local recurrence, and the disease-free survival at 5 years is almost 0% (1,2).

Complete surgical resection followed by radiation therapy offers the best chance of long-term control for chordoma. However, incomplete resection of the primary tumor makes controlling the disease more difficult and increases the odds of recurrence. Tumors at certain sites such as skull base chordoma can hardly be removed completely due to the complicated peritumoral tissue structure which makes the tumor difficult to be exposed. Thus, recurrence of skull base chordoma is as high as 85%. Chordomas are relatively radioresistant as well, requiring high doses of radiation to be controlled. The proximity of chordomas to vital neurological structures such as the brain stem and nerves limits the dose of radiation that can safely be delivered. A strategy to control the recurrence of chordomas is vital for improving the survival rate of patients. It is imperative to explore chordoma recurrence mechanisms at the molecular level and to search for alternative therapeutic methods including chemotherapy to treat it. Recently, Zhou *et al* assessed the chordoma proteome in chordoma tumor tissues and identified ENO1, PKM2, and gp96 proteins as being upregulated in chordomas. They reported that the expression of these proteins was higher in recurrent than that in the primary chordomas (3). However, the molecular mechanisms involved in chordoma recurrence remain unstudied, and the detailed changes in proteomic profiling in the process of recurrence remain unclear.

We analyzed 3,296 proteins identified by mass spectrum in a chordoma patient original tumor (CSO) and recurrent tumor (CSR) tissue. Bioconductor's Global Anova test was applied to compare the overall proteomic profiling changes between CSO and CSR which indicated there was a significant difference ($P \leq 0.1$). Bioconductor's multtest found that 359 proteins exhibited the highest expression difference between CSO and CSR. KEGG database analysis of the 359 proteins revealed that 21 pathways had a significant change between CSO and CSR. Immunohistochemistry (IHC) further verified that cancer stem cell marker activated leukocyte cell adhesion molecule (ALCAM or CD166) was markedly upregulated in the CSR tissue.

Correspondence to: Professor Jianru Xiao, Department of Bone Tumor Surgery, Changzheng Hospital, Second Military Medical University, 415 Fengyang Road, Shanghai 200003, P.R. China
E-mail: jrx_cz@163.com

*Contributed equally

Key words: proteome, chordomas, bioinformation, ALCAM

Materials and methods

Tissue specimen processing. Chordoma specimens were obtained from a resected tumor following an institutional review board approved protocol. The histological composition of the samples was assessed by examining adjacent sections. Tumor samples were dissected and only tissue that was superfluous to that required for pathological evaluation was taken. The samples were immediately snap-frozen in liquid nitrogen and stored at -80˚C. Approximately 800 μg of tissue samples was cut into small pieces with a scalpel and transferred into a mortar filled with liquid nitrogen. The tissue was ground to a fine powder with a pestle in the continuous presence of liquid nitrogen and transferred into a reaction tube with extraction buffer [2 M thiocarbamide, 7 M urea and 10 μM proteinase inhibitor (Roche Diagnostics, Indianapolis, IN, USA)] at 4˚C. The solution was centrifuged at 16,000 x g at 4˚C for 15 min, and the supernatant (~300-400 μl) was stored frozen at -200˚C.

Proteome analysis. The protein concentration was determined by Amersham 2D Quant kit (GE Healthcare Bio-Sciences, Piscataway, NJ, USA). The protein samples were further lysed to peptides and prepared for proteome analysis as described previously (4). Peptides were analyzed using strong cation (SCX)/reversed phase, upgrade performance liquid chromatography (Nano-RPLC)/ESI/MS/MS. Samples were analyzed using a LTQ Orbitrap XL (Thermo Electron Corp., Bremen, Germany) mass spectrometer. MS/MS spectra data were searched against the Swiss-Prot Human (2009.02.10, 20331 sequences) database or IPI database using Bioworks Browser 3.3.1 SP1. The identified proteins were quantified by APEX software (5,6). To control the false-positive rate, finally the quantitative results by false-discovery rate (FDR) 1% or less (false-positive rate of 1% or less) as the standard filter.

Immunohistochemistry. The paraffin sections were dried in an oven at 65˚C for 1 h. The paraffin sections were then dewaxed in xylene and rehydrated in a series of ethanol solutions. The endogenous peroxidase activity was blocked by a 10-min pre-incubation with 3% H_2O_2. The paraffin sections were preheated at 100˚C in antigen retrieval solution containing EDTA (pH 8.0) for 30 min and blocked by non-immune goat serum at room temperature for 15 min to decrease unspecific staining. Incubation with mouse polyclonal anti-ALCAM (1:1,000 dilution) was performed overnight at 4˚C. After being washed 3 times with 1X PBS buffer for 3 min, the sections were incubated with the secondary (link) antibody (biotinylated mouse-anti-human IgG) for 30 min at room temperature. After reacting with the streptavidin-biotin-peroxidase complex for 20 min, the immunoreactivity was determined by 3,3'-diamino-benzidine tetrahydrochloride and H_2O_2 at room temperature according to the manufacturer's instructions. The positive reaction was manifested as brown (DAB) staining. The sections were counterstained in Mayer's hematoxylin. The selected sections were scanned at x400 magnification to visualize the localization and distribution of ALCAM.

Statistical analysis. Statistically significant proteins were identified by first performing a two-tailed Student's t-test with the 'multtest' package in rat the respective time-points by comparing protein abundance between CSO and CSR. Multiple hypothesis testing was then implemented with the 'rawp2adjp' function in R by correcting the P-values according to Benjamini and Hochberg procedures (7) to control the FDRs to ≤1%. Proteins with a FDR ≤1%, peptide count ≥3, and fold-change ≥2 were identified as statistically significant. Throughout the present study, upregulation is defined as higher protein abundance measured in CSR relative to CSO and downregulation refers to fewer proteins measured with CSR. Moreover, a positive expression ratio represents upregulation and negative represents downregulation. Blast2Go (8) was used as a comprehensive bioinformatics tool for the functional annotation of the protein sequences in the present study such as determining gene ontology terms. The metabolic map at CSR was generated by first using the statistically significant proteins to identify the key pathways. Once the pathways were identified, all of the detected proteins in the same pathway were evaluated to determine whether they were upregulated or downregulated relative to the control. If ≥50% of the proteins in the pathway was regulated similarly in the same direction, then the pathway would be designated as upregulated or downregulated according to the majority. The cellular pathways are displayed using the iPath 2.0 platform (9).

Results and Discussion

In order to obtain a comprehensive proteomic profile of CSO and CSR and to investigate the mechanism of recurrence, the proteome of patient CSO and CSR tumor tissue samples was analyzed with LC/MS. In total, 3,296 unique protein sequences were identified. Bioconductor's Global Anova package was used to determine the significance of the protein expression change between CSO and CSR. A protein expression difference with P≤0.1±0.002 was defined as statistically significant (Table I). Furthermore, we applied Bioconductor's multtest package to analyze the identified 3,296 proteins and found that a large number of proteins (359) showed significant changes in expression with BH ≤0.01 and P≤0.01 between CSO and CSR. These proteins were involved in central metabolism, genetic information transcription and other processes essential to cell functions. Of these 359 proteins, there were 244 downregulated proteins (CSR/CSO value ≤0.1) and 115 upregulated proteins (CSR/CSO ≥9) (Fig. 1; Table III and IV). This analysis discovered many significant proteins which have never been reported before in recurrent chordomas.

Among the top downregulated proteins, podocan is involved in negative regulation of cell migration and proliferation, concomitant with increased p21 expression which is a tumor-suppressor gene and can mediate cellular senescence (10). ZO-1 has been shown to be downregulated in poorly differentiated, highly invasive breast cancer cell lines (11), and downregulation of complement factor I (CFI) is regarded as a potential suppressive protein for gastric cancer identified by serum proteome analysis (12). Downregulation of osteomodulin (OMD) is referred to in the context of uterine serous papillary carcinoma. It was further disclosed that activation of OMD or/and PRELP gene expression or function can suppress cancer initiation and development (13). FK506-binding protein 4 (FKBP4) was reported to have cancer-specific methylation which usually inactivates this

Table I. Global test for differential gene expression.

ANOVA	SSQ	DF	MS
Effect	0.002073207	3296	6.29007E-07
Error	0.00065985	13184	5.00493E-08
Test Result			
F.value	12.56774798		
p.perm	0.1		
p.approx	0.002139239		

*p≤0.1.

Table II. KEGG database identified 21 pathways with Seqs ≥3.

Pathways	#Seqs	#Enzs
Purine metabolism	10	11
Arginine and proline metabolism	5	6
Starch and sucrose metabolism	5	6
Pyruvate metabolism	4	4
Glycolysis/gluconeogenesis	4	4
Oxidative phosphorylation	4	2
Alanine, aspartate and glutamate metabolism	4	5
Cysteine and methionine metabolism	4	5
Aminoacyl-tRNA biosynthesis	3	3
Butanoate metabolism	3	3
Methane metabolism	3	3
Streptomycin biosynthesis	3	3
Amino sugar and nucleotide sugar metabolism	3	5
Propanoate metabolism	3	4
Valine, leucine and isoleucine degradation	3	3
β-alanine metabolism	3	4
Drug metabolism - other enzymes	3	2
Glyoxylate and dicarboxylate metabolism	3	3
Phosphatidylinositol signaling system	3	3
Inositol phosphate metabolism	3	3
Pyrimidine metabolism	3	3

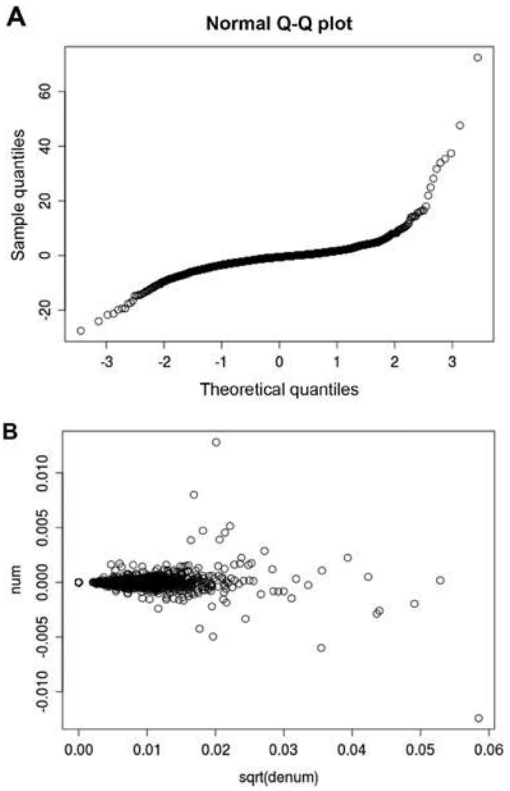

Figure 1. (A) Normal Q-Q plot of t-statistics for the protein data. The points that deviate markedly from an otherwise linear relationship correspond to those genes whose expression levels differ between the CSO and CSR groups. (B) Numerator vs. square root of denominator of the t-statistics for the protein data. The majority of proteins which do not reveal any difference in expression between CSO and CSR groups are represented by points distributed on the y-axis around zero. Some of the points that deviate from this area represent the corresponding proteins whose expression levels are higher or lower in the CSR group than that in the CSO group. CSO, chordoma primary tumor; CSR, recurrent tumor.

gene in breast cancer tissues (14). We are the first to report downregulation of these tumor-suppressing proteins in recurrent chordomas. The markedly decreased expression of these tumor-suppressing proteins suggests that recurrent chordomas are more aggressive than primary chordomas. While the top upregulated proteins included myosin-7 (MYH7) which is related to eukaryotic cell motility; CD166 (ALCAM) has been regarded as a potential cancer stem cell marker (15). Splicing factor, arginine/serine-rich 2 (SFRS2) demonstrated Wnt signaling-dependent activation which promotes cell migration (16); and Ras-related protein Rab-11A (RAB11A) can differentially modulate epidermal growth factor-induced proliferation and motility in immortal breast cells (17). These newly identified upregulated molecules in recurrent chordomas by our analysis may be possible biomarkers for diagnosis and/or targets for treating recurrent chordomas. Our study also provides valuable information for future studies on chordoma recurrence mechanisms which remain unelucidated.

To investigate which signaling pathways have alterations in CSR, we searched the 359 identified proteins with significant change in the KEGG database and found that there were over 21 pathways with Seqs ≥3 between CSO and CSR as shown in Table II. Eight pathways were markedly upregulated in CSR compared with CSO (num upregulated protein ≥60%) and nine pathways were apparently downregulated in CSR compared with CSO (num downregulated protein ≥60%) (Fig. 2). Notably, most of the upregulated pathways (6 of 8) and cellular components are involved in carbohydrate metabolism indicating that carbohydrate metabolic activity was higher in recurrent chordomas than in primary chordomas (Fig. 2). Fig. 3 shows that the top 3 upregulated pathways including butanoate, inositol phosphate and glyoxylate and dicarboxylate metabolism are all involved in carbohydrate metabolism. Those 3 pathways were upregulated by 85.7, 75 and 73.3%, respectively, in the CSR compared with the CSO (Fig. 3). The glycolysis/gluconeogenesis pathway was also upregulated (Fig. 2). It has been reported that a high glycolytic rate has advantages for malignant cells (18). High glycolytic activity produces high levels of lactate and H^+ ions which are transported outside the cell where they directly promote tumor aggressiveness through invasion and metastasis, two other hallmarks of cancer (19). Additionally, the genes and pathways that upregulate

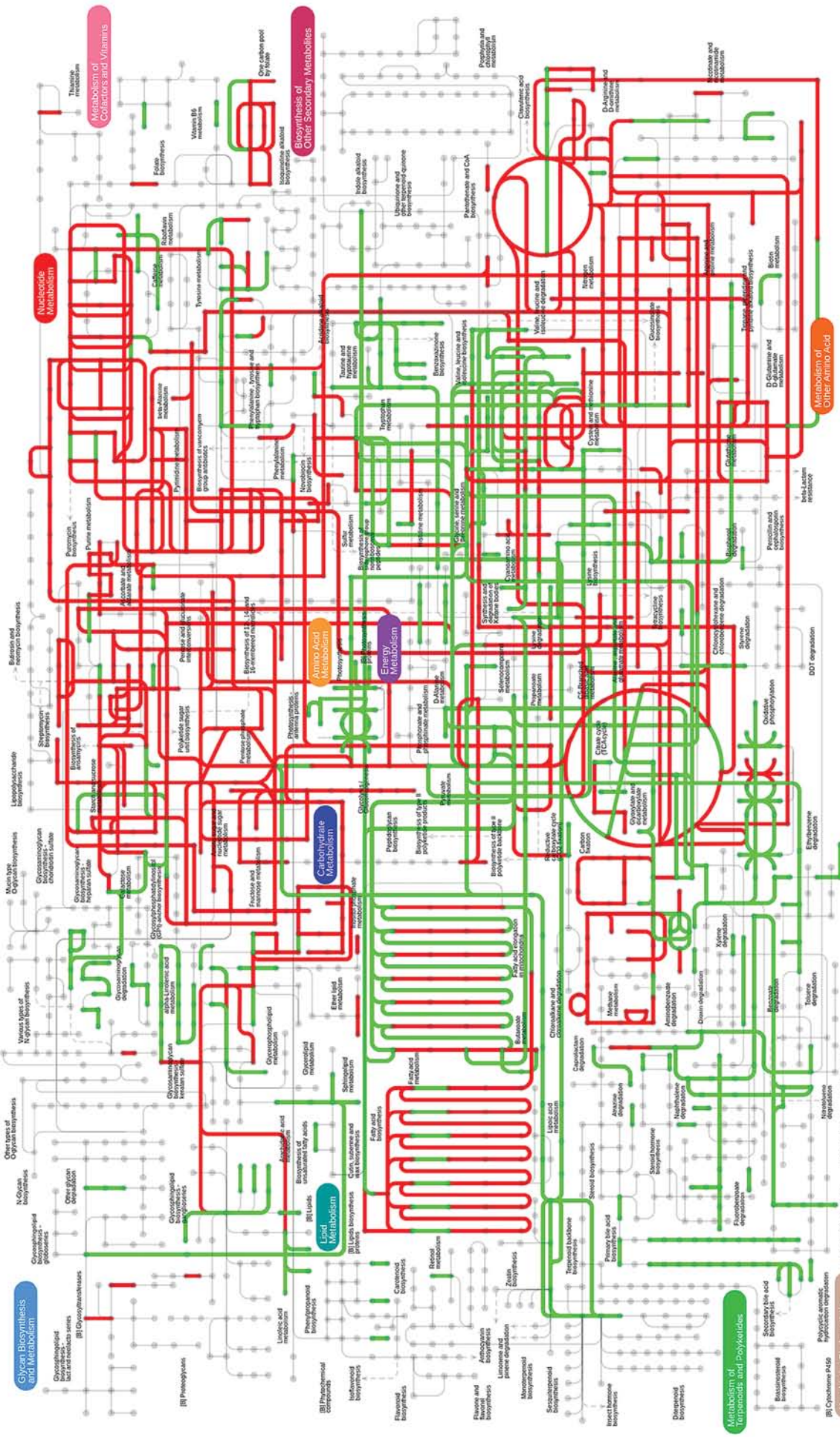

Figure 2. An overview of how the metabolic pathways were changed between CSO and CSR. Red color represents downregulation, green represents upregulation and grey represents no change. Key metabolic pathways are highlighted with bold font. CSO, chordoma primary tumor; CSR, recurrent tumor.

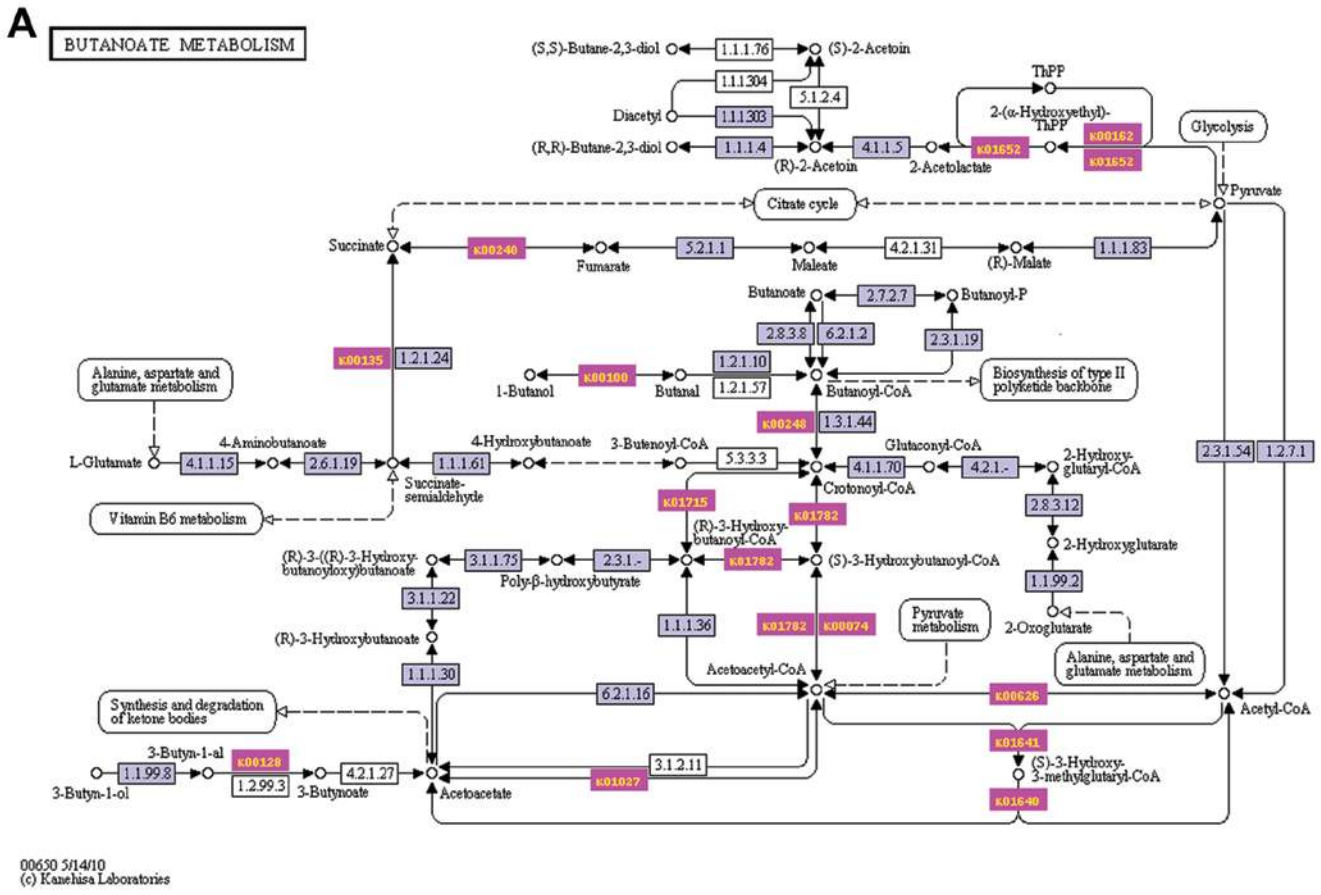

Figure 3. Top upregulated pathways in the KEGG database. (A) Carbohydrate metabolism, butanoatemetabolism pathway. (B) Carbohydrate metabolism, inositol phosphate metabolism.

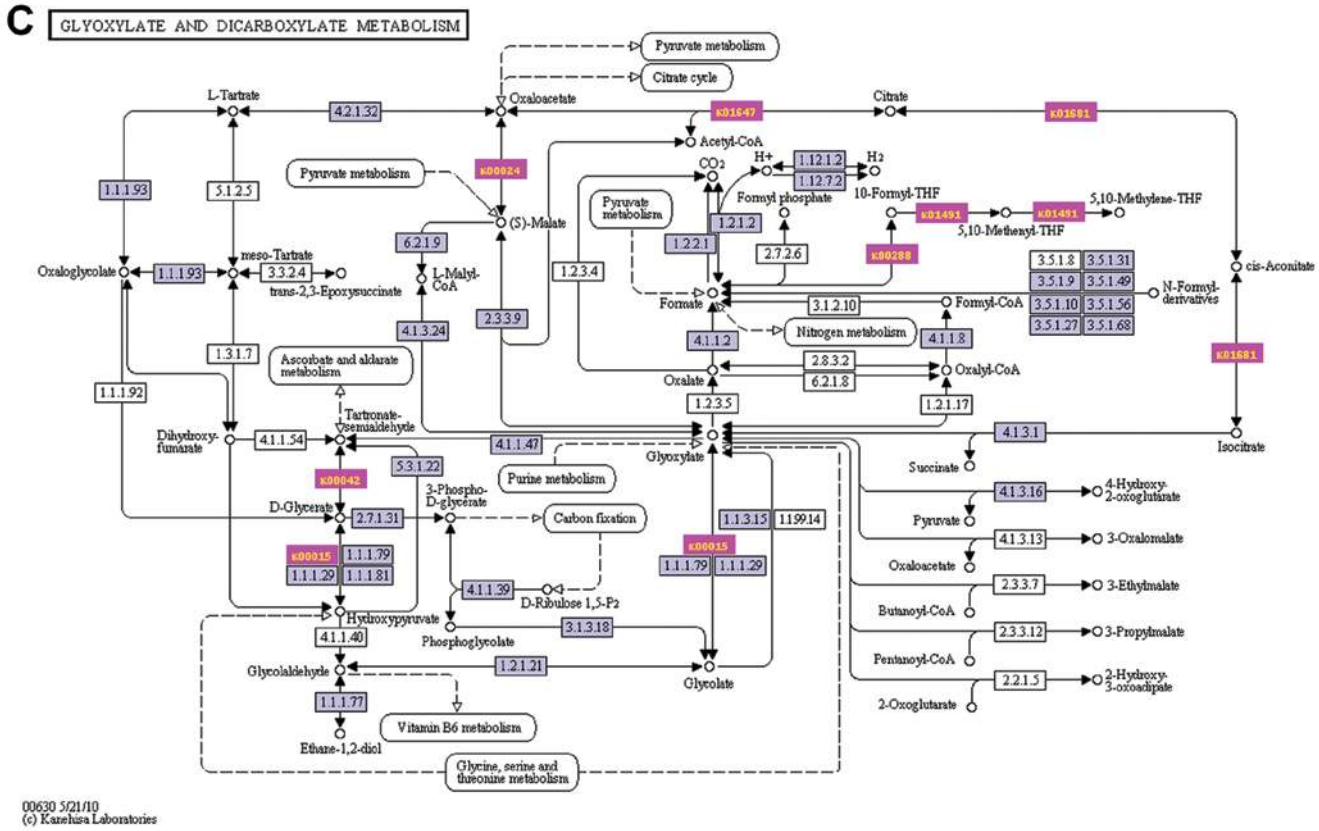

Figure 3. Continued. Top upregulated pathways in the KEGG database. (C) Carbohydrate metabolism, glyoxylate and dicarboxylate metabolism.

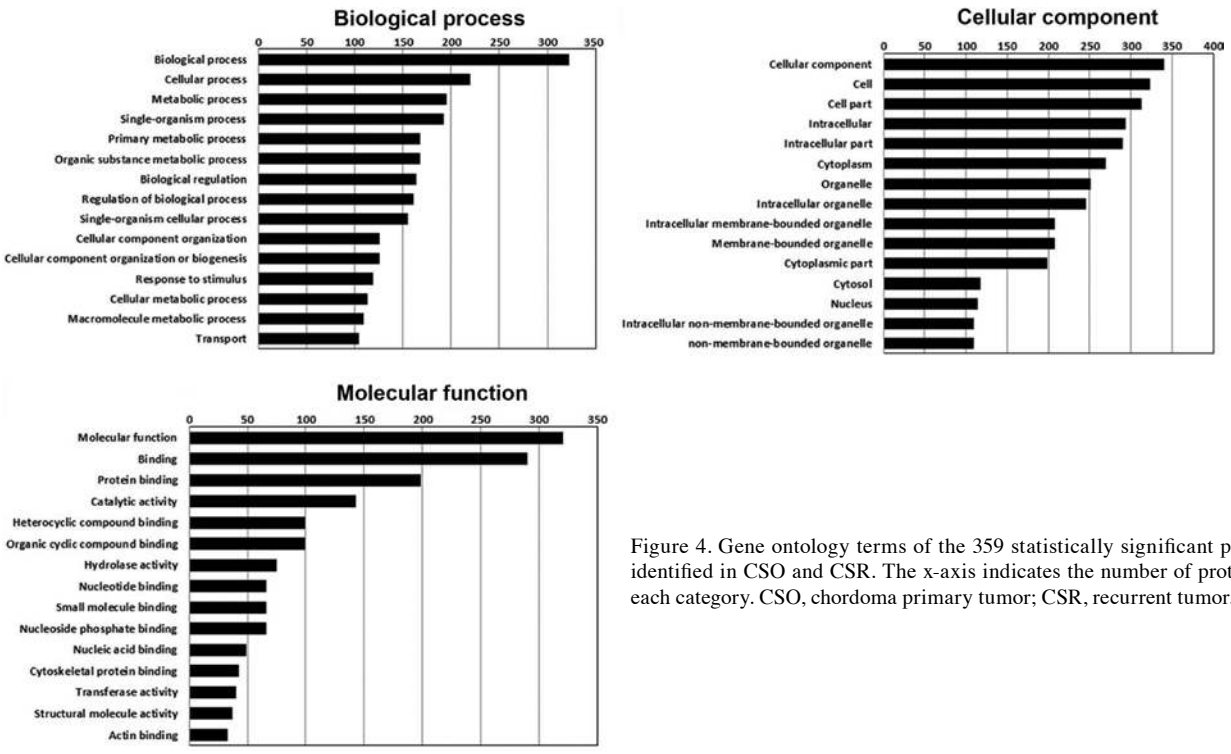

Figure 4. Gene ontology terms of the 359 statistically significant proteins identified in CSO and CSR. The x-axis indicates the number of proteins in each category. CSO, chordoma primary tumor; CSR, recurrent tumor.

glycolysis are themselves anti-apoptotic (20). The increased carbohydrate metabolism in recurrent chordomas suggests that recurrent chordomas have a more aggressive phenotype and are resistant to therapy. The other 2 upregulated pathways in the recurrent chordomas are involved in energy metabolism and amino acid metabolism. In contrast to the upregulated pathways, the downregulated pathways participate in various biological processes and molecular functions including

Table III. Downregulated proteins (244) (CSR/CSO value ≤0.1).

Protein	Protein_description
Q7Z5L7	Podocan GN=PODN
Q7L5N1	COP9 signalosome complex subunit 6 GN=COPS6
P31939	Bifunctional purine biosynthesis protein PURH GN=ATIC
O94808	Glucosamine-fructose-6-phosphate aminotransferase (isomerizing) 2 GN=GFPT2
Q8TD55	Pleckstrin homology domain-containing family O member 2 GN=PLEKHO2
O75400	Pre-mRNA-processing factor 40 homolog A GN=PRPF40A
Q6KB66	Keratin, type II cytoskeletal 80 GN=KRT80
Q07157	Tight junction protein ZO-1 GN=TJP1
P10155	60 kDa SS-A/Ro ribonucleoprotein GN=TROVE2
P05156	Complement factor I GN=CFI
Q99983	Osteomodulin GN=OMD
Q02790	FK506-binding protein 4 GN=FKBP4
Q9Y240	C-type lectin domain family 11 member A GN=CLEC11A
Q9H8Y8	Golgi reassembly-stacking protein 2 GN=GORASP2
P27658	Collagen α-1(VIII) chain GN=COL8A1
P27169	Serum paraoxonase/arylesterase 1 GN=PON1
Q99729	Heterogeneous nuclear ribonucleoprotein A/B GN=HNRNPAB
Q9H4A4	Aminopeptidase B GN=RNPEP
P50570	Dynamin-2 GN=DNM2
Q14157	Ubiquitin-associated protein 2-like GN=UBAP2L
P02788	Lactotransferrin GN=LTF
Q96S97	Myeloid-associated differentiation marker GN=MYADM
O60841	Eukaryotic translation initiation factor 5B GN=EIF5B
Q96C19	EF-hand domain-containing protein D2 GN=EFHD2
P50225	Sulfotransferase 1A1 GN=SULT1A1
A0AVT1	Ubiquitin-like modifier-activating enzyme 6 GN=UBA6
A0MZ66	Shootin-1 GN=KIAA1598
A1L4H1	Scavenger receptor cysteine-rich domain-containing protein LOC284297
A8MWD9	Small nuclear ribonucleoprotein G-like protein
O00154	Cytosolic acyl coenzyme A thioester hydrolase GN=ACOT7
O00461	Golgi integral membrane protein 4 GN=GOLIM4
O14791	Apolipoprotein L1 GN=APOL1
O43592	Exportin-T GN=XPOT
O43670	Zinc finger protein 207 GN=ZNF207
O43847	Nardilysin GN=NRD1
O60240	Perilipin GN=PLIN
O60684	Importin subunit α-7 GN=KPNA6
O60687	Sushi repeat-containing protein SRPX2 GN=SRPX2
O60831	PRA1 family protein 2 GN=PRAF2
O75094	Slit homolog 3 protein GN=SLIT3
O75110	Probable phospholipid-transporting ATPase IIA GN=ATP9A
O75339	Cartilage intermediate layer protein 1 GN=CILP
O75592	Probable E3 ubiquitin-protein ligase MYCBP2 GN=MYCBP2
O76021	Ribosomal L1 domain-containing protein 1

Table III. Continued.

Protein	Protein_description
O94769	Extracellular matrix protein 2 GN=ECM2
O94903	Proline synthetase co-transcribed bacterial homolog protein GN=PROSC
O95302	FK506-binding protein 9 GN=FKBP9
O95373	Importin-7 GN=IPO7
O95425	Supervillin GN=SVIL
O95433	Activator of 90 kDa heat shock protein ATPase homolog 1 GN=AHSA1
O95757	Heat shock 70 kDa protein 4L GN=HSPA4L
O95810	Serum deprivation-response protein GN=SDPR
O95816	BAG family molecular chaperone regulator 2 GN=BAG2
O95965	Integrin β-like protein 1 GN=ITGBL1
O96005	Cleft lip and palate transmembrane protein 1 GN=CLPTM1
P01614	Ig κ chain V-II region cum
P01781	Ig heavy chain V-III region GAL
P02724	Glycophorin-A GN=GYPA
P02750	Leucine-rich α-2-glycoprotein GN=LRG1
P04433	Ig κ chain V-III region VG (fragment)
P05543	Thyroxine-binding globulin GN=SERPINA7
P05546	Heparin cofactor 2 GN=SERPIND1
P07093	Glia-derived nexin GN=SERPINE2
P07358	Complement component C8 β chain GN=C8B
P08174	Complement decay-accelerating factor GN=CD55
P08253	72 kDa type IV collagenase GN=MMP2
P08493	Matrix Gla protein GN=MGP
P08708	40S ribosomal protein S17 GN=RPS17
P10253	Lysosomal α-glucosidase GN=GAA
P10451	Osteopontin GN=SPP1
P10600	Transforming growth factor β-3 GN=TGFB3
P11234	Ras-related protein Ral-B GN=RALB
P12004	Proliferating cell nuclear antigen GN=PCNA
P12107	Collagen α-1(XI) chain GN=COL11A1
P15104	Glutamine synthetase GN=GLUL
P19367	Hexokinase-1 GN=HK1
P20036	HLA class II histocompatibility antigen, DP α chain GN=HLA-DPA1
P20591	Interferon-induced GTP-binding protein Mx1 GN=MX1
P20851	C4b-binding protein β chain GN=C4BPB
P22102	Trifunctional purine biosynthetic protein adenosine-3 GN=GART
P23193	Transcription elongation factor A protein 1 GN=TCEA1
P23497	Nuclear autoantigen Sp-100 GN=SP100
P26373	60S ribosomal protein L13 GN=RPL13
P26599	Polypyrimidine tract-binding protein 1 GN=PTBP1
P26639	Threonyl-tRNA synthetase, cytoplasmic GN=TARS
P28300	Protein-lysine 6-oxidase GN=LOX
P31153	S-adenosylmethionine synthetase isoform type-2 GN=MAT2A
P32321	Deoxycytidylate deaminase GN=DCTD
P35542	Serum amyloid A-4 protein GN=SAA4
P35625	Metalloproteinase inhibitor 3 GN=TIMP3
P35858	Insulin-like growth factor-binding protein complex acid labile chain GN=IGFALS
P36969	Phospholzipid hydroperoxide glutathione peroxidase, mitochondrial GN=GPX4

Table III. Continued.

Protein	Protein_description
P39023	60S ribosomal protein L3 GN=RPL3
P41218	Myeloid cell nuclear differentiation antigen GN=MNDA
P41240	Tyrosine-protein kinase CSK GN=CSK
P45877	Peptidyl-prolyl *cis-trans* isomerase C GN=PPIC
P46108	Proto-oncogene C-crk GN=CRK
P46109	Crk-like protein GN=CRKL
P48556	26S proteasome non-ATPase regulatory subunit 8 GN=PSMD8
P49321	Nuclear autoantigenic sperm protein GN=NASP
P49354	Protein farnesyltransferase/geranylgeranyltransferase type-1 subunit α GN=FNTA
P49458	Signal recognition particle 9 kDa protein GN=SRP9
P49591	Seryl-tRNA synthetase, cytoplasmic GN=SARS
P50135	Histamine N-methyltransferase GN=HNMT
P50479	PDZ and LIM domain protein 4 GN=PDLIM4
P50583	Bis (5'-nucleosyl)-tetraphosphatase (asymmetrical) GN=NUDT2
P51148	Ras-related protein Rab-5C GN=RAB5C
P51812	Ribosomal protein S6 kinase α-3 GN=RPS6KA3
P52788	Spermine synthase GN=SMS
P55039	Developmentally-regulated GTP-binding protein 2 GN=DRG2
P55196	Afadin GN=MLLT4
P55212	Caspase-6 GN=CASP6
P60983	Glia maturation factor β GN=GMFB
P61221	ATP-binding cassette sub-family E member 1 GN=ABCE1
P61225	Ras-related protein Rap-2b GN=RAP2B
P61313	60S ribosomal protein L15 GN=RPL15
P61758	Prefoldin subunit 3 GN=VBP1
P61970	Nuclear transport factor 2 GN=NUTF2
P62195	26S protease regulatory subunit 8 GN=PSMC5
P62266	40S ribosomal protein S23 GN=RPS23
P62277	40S ribosomal protein S13 GN=RPS13
P62280	40S ribosomal protein S11 GN=RPS11
P62304	Small nuclear ribonucleoprotein E GN=SNRPE
P62316	Small nuclear ribonucleoprotein Sm D2 GN=SNRPD2
P62750	60S ribosomal protein L23a GN=RPL23A
P62847	40S ribosomal protein S24 GN=RPS24
P62857	40S ribosomal protein S28 GN=RPS28
P62899	60S ribosomal protein L31 GN=RPL31
P80217	Interferon-induced 35 kDa protein GN=IFI35
P80303	Nucleobindin-2 GN=NUCB2
P82987	ADAMTS-like protein 3 GN=ADAMTSL3
P83110	Probable serine protease HTRA3 GN=HTRA3
Q00341	Vigilin GN=HDLBP
Q03518	Antigen peptide transporter 1 GN=TAP1
Q04446	1,4-α-glucan-branching enzyme GN=GBE1
Q06124	Tyrosine-protein phosphatase non-receptor type 11 GN=PTPN11
Q08J23	tRNA (cytosine-5-)-methyltransferase NSUN2 GN=NSUN2
Q12965	Myosin-Ie GN=MYO1E
Q13123	Protein Red GN=IK
Q13315	Serine-protein kinase ATM GN=ATM
Q13838	Spliceosome RNA helicase BAT1 GN=BAT1
Q14011	Cold-inducible RNA-binding protein GN=CIRBP

Table III. Continued.

Protein	Protein_description
Q14558	Phosphoribosyl pyrophosphate synthetase-associated protein 1 GN=PRPSAP1
Q14699	Raftlin GN=RFTN1
Q15008	26S proteasome non-ATPase regulatory subunit 6 GN=PSMD6
Q15121	Astrocytic phosphoprotein PEA-15 GN=PEA15
Q15181	Inorganic pyrophosphatase GN=PPA1
Q15465	Sonic hedgehog protein GN=SHH
Q15907	Ras-related protein Rab-11B GN=RAB11B
Q3LXA3	Dihydroxyacetone kinase GN=DAK
Q3ZCW2	Galectin-related protein GN=GRP
Q5KU26	Collectin-12 GN=COLEC12
Q5TC82	Roquin GN=RC3H1
Q66K74	Microtubule-associated protein 1S GN=MAP1S
Q6ZVZ8	Ankyrin repeat and SOCS box-containing protein 18 GN=ASB18
Q7Z304	MAM domain-containing protein 2 GN=MAMDC2
Q7Z333	Probable helicase senataxin GN=SETX
Q86UE8	Serine/threonine-protein kinase tousled-like 2 GN=TLK2
Q86W92	Liprin-β-1 GN=PPFIBP1
Q86X55	Histone-arginine methyltransferase CARM1 GN=CARM1
Q8IWE2	Protein NOXP20 GN=FAM114A1
Q8IWU6	Extracellular sulfatase Sulf-1 GN=SULF1
Q8IXB1	DnaJ homolog subfamily C member 10 GN=DNAJC10
Q8IXM2	Uncharacterized potential DNA-binding protein C17orf49 GN=C17orf49
Q8N129	Protein canopy homolog 4 GN=CNPY4
Q8N573	Oxidation resistance protein 1 GN=OXR1
Q8N6Q3	CD177 antigen GN=CD177
Q8NB37	Parkinson disease 7 domain-containing protein 1 GN=PDDC1
Q8TDX7	Serine/threonine-protein kinase Nek7 GN=NEK7
Q8WWI1	LIM domain only protein 7 GN=LMO7
Q92673	Sortilin-related receptor GN=SORL1
Q92696	Geranylgeranyl transferase type-2 subunit α GN=RABGGTA
Q92882	Osteoclast-stimulating factor 1 GN=OSTF1
Q93009	Ubiquitin carboxyl-terminal hydrolase 7 GN=USP7
Q96AT9	Ribulose-phosphate 3-epimerase GN=RPE
Q96C23	Aldose 1-epimerase GN=GALM
Q96CG8	Collagen triple helix repeat-containing protein 1 GN=CTHRC1
Q96CV9	Optineurin GN=OPTN
Q96FW1	Ubiquitin thioesterase OTUB1 GN=OTUB1
Q96GS4	Uncharacterized protein C17orf59 GN=C17orf59
Q96HF1	Secreted frizzled-related protein 2 GN=SFRP2
Q96HN2	Putative adenosylhomocysteinase 3 GN=AHCYL2
Q96JB1	Dynein heavy chain 8, axonemal GN=DNAH8
Q96JQ2	Calmin GN=CLMN
Q96MM6	Heat shock 70 kDa protein 12B GN=HSPA12B
Q96N66	Membrane-bound O-acyltransferase domain-containing protein 7 GN=MBOAT7
Q96PX9	Pleckstrin homology domain-containing family G member 4B GN=PLEKHG4B
Q96RF0	Sorting nexin-18 GN=SNX18
Q96RL7	Vacuolar protein sorting-associated protein 13A GN=VPS13A

Table III. Continued.

Protein	Protein_description
Q99426	Tubulin folding cofactor B GN=TBCB
Q99538	Legumain GN=LGMN
Q99622	Protein C10 GN=C12orf57
Q99627	COP9 signalosome complex subunit 8 GN=COPS8
Q9BRG1	Vacuolar protein-sorting-associated protein 25 GN=VPS25
Q9BUT1	3-hydroxybutyrate dehydrogenase type 2 GN=BDH2
Q9BVJ7	Dual specificity protein phosphatase 23 GN=DUSP23
Q9BXJ0	Complement C1q tumor necrosis factor-related protein 5 GN=C1QTNF5
Q9BXP5	Arsenite-resistance protein 2 GN=ARS2
Q9BXS5	AP-1 complex subunit mu-1 GN=AP1M1
Q9BY32	Inosine triphosphate pyrophosphatase GN=ITPA
Q9H0W9	Ester hydrolase C11orf54 GN=C11orf54
Q9H2D6	TRIO and F-actin-binding protein GN=TRIOBP
Q9H488	GDP-fucose protein O-fucosyltransferase 1 GN=POFUT1
Q9H6V9	UPF0554 protein C2orf43 GN=C2orf43
Q9HAB8	Phosphopantothenate-cysteine ligase GN=PPCS
Q9HB40	Retinoid-inducible serine carboxypeptidase GN=SCPEP1
Q9HCJ1	Progressive ankylosis protein homolog GN=ANKH
Q9NQR4	Nitrilase homolog 2 GN=NIT2
Q9NRN5	Olfactomedin-like protein 3 GN=OLFML3
Q9NS15	Latent-transforming growth factor β-binding protein 3 GN=LTBP3
Q9NZL9	Methionine adenosyltransferase 2 subunit β GN=MAT2B
Q9P258	Protein RCC2 GN=RCC2
Q9UBB6	Neurochondrin GN=NCDN
Q9UBR2	Cathepsin Z GN=CTSZ
Q9UBW8	COP9 signalosome complex subunit 7α GN=COPS7A
Q9UDY2	Tight junction protein ZO-2 GN=TJP2
Q9UEY8	γ-adducin GN=ADD3
Q9UHL4	Dipeptidyl-peptidase 2 GN=DPP7
Q9UHY7	Enolase-phosphatase E1 GN=ENOPH1
Q9UJC5	SH3 domain-binding glutamic acid-rich-like protein 2 GN=SH3BGRL2
Q9UKU9	Angiopoietin-related protein 2 GN=ANGPTL2
Q9UM19	Hippocalcin-like protein 4 GN=HPCAL4
Q9UM47	Neurogenic locus notch homolog protein 3 GN=NOTCH3
Q9UM54	Myosin-VI GN=MYO6
Q9UMS0	NFU1 iron-sulfur cluster scaffold homolog, mitochondrial GN=NFU1
Q9UNF0	Protein kinase C and casein kinase substrate in neurons protein 2 GN=PACSIN2
Q9UNH6	Sorting nexin-7 GN=SNX7
Q9UPN7	Serine/threonine-protein phosphatase 6 regulatory subunit 1 GN=SAPS1
Q9Y266	Nuclear migration protein nudC GN=NUDC
Q9Y287	Integral membrane protein 2B GN=ITM2B
Q9Y3C6	Peptidyl-prolyl *cis-trans* isomerase-like 1 GN=PPIL1
Q9Y4E8	Ubiquitin carboxyl-terminal hydrolase 15 GN=USP15
Q9Y5K8	V-type proton ATPase subunit D GN=ATP6V1D
Q9Y5U9	Immediate early response 3-interacting protein 1 GN=IER3IP1
Q9Y5X1	Sorting nexin-9 GN=SNX9
Q9Y5X3	Sorting nexin-5 GN=SNX5
Q9Y6K5	2'-5'-Oligoadenylate synthetase 3 GN=OAS3
Q9Y6R7	IgGFc-binding protein GN=FCGBP
O43765	Small glutamine-rich tetratricopeptide repeat-containing protein α GN=SGTA
O60749	Sorting nexin-2 GN=SNX2
Q12765	Secernin-1 GN=SCRN1
Q8N0U8	Vitamin K epoxide reductase complex subunit 1-like protein 1 GN=VKORC1L1
Q9NYL4	FK506-binding protein 11 GN=FKBP11

Table IV. Upregulated proteins (115).

Protein	Protein_description
O00148	ATP-dependent RNA helicase DDX39 GN=DDX39
O00330	Pyruvate dehydrogenase protein X component, mitochondrial GN=PDHX
O00629	Importin subunit α-4 GN=KPNA4
O00748	Carboxylesterase 2 GN=CES2
O14958	Calsequestrin-2 GN=CASQ2
O43676	NADH dehydrogenase (ubiquinone) 1 β subcomplex subunit 3 GN=NDUFB3
O60784	Target of Myb protein 1 GN=TOM1
O75112	LIM domain-binding protein 3 GN=LDB3
O75128	Protein cordon-bleu GN=COBL
O75298	Reticulon-2 GN=RTN2
O75306	NADH dehydrogenase (ubiquinone) iron-sulfur protein 2, mitochondrial GN=NDUFS2
O94826	Mitochondrial import receptor subunit TOM70 GN=TOMM70A
O94906	Pre-mRNA-processing factor 6 GN=PRPF6
O94925	Glutaminase kidney isoform, mitochondrial GN=GLS
O95248	Myotubularin-related protein 5 GN=SBF1
O95299	NADH dehydrogenase (ubiquinone) 1 α subcomplex subunit 10, mitochondrial GN=NDUFA10
P02585	Troponin C, skeletal muscle GN=TNNC2
P05166	Propionyl-CoA carboxylase β chain, mitochondrial GN=PCCB
P06732	Creatine kinase M-type GN=CKM
P07451	Carbonic anhydrase 3 GN=CA3
P08590	Myosin light chain 3 GN=MYL3
P10916	Myosin regulatory light chain 2, ventricular/cardiac muscle isoform GN=MYL2
P11217	Glycogen phosphorylase, muscle form GN=PYGM
P11233	Ras-related protein Ral-A GN=RALA
P13805	Troponin T, slow skeletal muscle GN=TNNT1
P13807	Glycogen (starch) synthase, muscle GN=GYS1
P14649	Myosin light chain 6B GN=MYL6B
P19237	Troponin I, slow skeletal muscle GN=TNNI1
P23327	Sarcoplasmic reticulum histidine-rich calcium-binding protein GN=HRC
P28289	Tropomodulin-1 GN=TMOD1
P29218	Inositol monophosphatase GN=IMPA1
P30038	δ-1-pyrroline-5-carboxylate dehydrogenase, mitochondrial GN=ALDH4A1
P31513	Dimethylaniline monooxygenase (N-oxide-forming) 3 GN=FMO3

Table IV. Continued.

Protein	Protein_description
P35080	Profilin-2 GN=PFN2
P35609	α-actinin-2 GN=ACTN2
P42704	Leucine-rich PPR motif-containing protein, mitochondrial GN=LRPPRC
P45378	Troponin T, fast skeletal muscle GN=TNNT3
P48788	Troponin I, fast skeletal muscle GN=TNNI2
P50461	Cysteine and glycine-rich protein 3 GN=CSRP3
P51553	Isocitrate dehydrogenase (NAD) subunit γ, mitochondrial GN=IDH3G
P52179	Myomesin-1 GN=MYOM1
P54296	Myomesin-2 GN=MYOM2
P63316	Troponin C, slow skeletal and cardiac muscles GN=TNNC1
Q00872	Myosin-binding protein C, slow-type GN=MYBPC1
Q02045	Myosin light chain 5 GN=MYL5
Q09013	Myotonin-protein kinase GN=DMPK
Q10589	Bone marrow stromal antigen 2 GN=BST2
Q13061	Triadin GN=TRDN
Q14118	Dystroglycan GN=DAG1
Q14324	Myosin-binding protein C, fast-type GN=MYBPC2
Q15111	Inactive phospholipase C-like protein 1 GN=PLCL1
Q16630	Cleavage and polyadenylation specificity factor subunit 6 GN=CPSF6
Q16775	Hydroxyacylglutathione hydrolase GN=HAGH
Q5BKX8	PTRF/SDPR family protein
Q5T1J5	Coiled-coil-helix-coiled-coil-helix domain-containing protein 9, mitochondrial GN=CHCHD9
Q5VTT5	Myomesin-3 GN=MYOM3
Q5VXT5	Synaptophysin-like protein 2 GN=SYPL2
Q5W0V3	UPF0518 protein FAM160B1 GN=FAM160B1
Q6ZMU5	Tripartite motif-containing protein 72 GN=TRIM72
Q702N8	Xin actin-binding repeat-containing protein 1 GN=XIRP1
Q86TD4	Sarcalumenin GN=SRL
Q86UW8	Hyaluronan and proteoglycan link protein 4 GN=HAPLN4
Q86VU5	Catechol-O-methyltransferase domain-containing protein 1 GN=COMTD1
Q8IWX7	Protein unc-45 homolog B GN=UNC45B
Q8IZL8	Proline-, glutamic acid- and leucine-rich protein 1 GN=PELP1
Q8N1G4	Leucine-rich repeat-containing protein 47 GN=LRRC47
Q8NE86	Coiled-coil domain-containing protein 109A GN=CCDC109A
Q8NF37	1-acylglycerophosphocholine O-acyltransferase 1 GN=LPCAT1
Q8NFW1	Collagen α-1(XXII) chain GN=COL22A1
Q8NI60	Chaperone activity of bc1 complex-like, mitochondrial GN=CABC1
Q8WW22	DnaJ homolog subfamily A member 4 GN=DNAJA4
Q92629	δ-sarcoglycan GN=SGCD
Q96A32	Myosin regulatory light chain 2, skeletal muscle isoform GN=MYLPF
Q96EY8	Cob(I)yrinic acid a,c-diamide adenosyltransferase, mitochondrial GN=MMAB
Q9BQS8	FYVE and coiled-coil domain-containing protein 1 GN=FYCO1
Q9BWD1	Acetyl-CoA acetyltransferase, cytosolic GN=ACAT2
Q9GZV1	Ankyrin repeat domain-containing protein 2 GN=ANKRD2
Q9HC07	Transmembrane protein 165 GN=TMEM165
Q9NP98	Myozenin-1 GN=MYOZ1
Q9NPC6	Myozenin-2 GN=MYOZ2
Q9NTI5	Sister chromatid cohesion protein PDS5 homolog B GN=PDS5B
Q9NZQ9	Tropomodulin-4 GN=TMOD4
Q9UBF9	Myotilin GN=MYOT
Q9UKS6	Protein kinase C and casein kinase substrate in neurons protein 3 GN=PACSIN3
Q9Y235	Probable C-)U-editing enzyme APOBEC-2 GN=APOBEC2
Q9Y2J8	Protein-arginine deiminase type-2 GN=PADI2
Q9Y639	Neuroplastin GN=NPTN
P12883	Myosin-7 GN=MYH7
P31415	Calsequestrin-1 GN=CASQ1
P20929	Nebulin GN=NEB
Q8WZ42	Titin GN=TTN
P05976	Myosin light chain 1, skeletal muscle isoform GN=MYL1
P02144	Myoglobin GN=MB
P11532	Dystrophin GN=DMD
Q14315	Filamin-C GN=FLNC
Q9UHQ9	NADH-cytochrome b5 reductase 1 GN=CYB5R1
Q9NZ01	Synaptic glycoprotein SC2 GN=GPSN2
Q13740	CD166 antigen GN=ALCAM
O95817	BAG family molecular chaperone regulator 3 GN=BAG3
P25786	Proteasome subunit α type-1 GN=PSMA1
Q01130	Splicing factor, arginine/serine-rich 2 GN=SFRS2
P12235	ADP/ATP translocase 1 GN=SLC25A4
P13929	β-enolase GN=ENO3
O75923	Dysferlin GN=DYSF
P53634	Dipeptidyl-peptidase 1 GN=CTSC
P23258	Tubulin γ-1 chain GN=TUBG1
O75746	Calcium-binding mitochondrial carrier protein Aralar1 GN=SLC25A12
O94919	Endonuclease domain-containing 1 protein GN=ENDOD1
P24043	Laminin subunit α-2 GN=LAMA2
P11216	Glycogen phosphorylase, brain form GN=PYGB
P12829	Myosin light chain 4 GN=MYL4
P55042	GTP-binding protein RAD GN=RRAD
P62491	Ras-related protein Rab-11A GN=RAB11A
Q14BN4	Sarcolemmal membrane-associated protein GN=SLMAP
Q96JG9	Zinc finger protein 469 GN=ZNF469

nucleotide metabolism, amino acid metabolism, carbohydrate metabolism, genetic information processing and translation, and biosynthesis of other secondary metabolites.

To further determine the cellular function change between CSO and CRO, the statistically significant 359 proteins identified were classified according to gene ontology

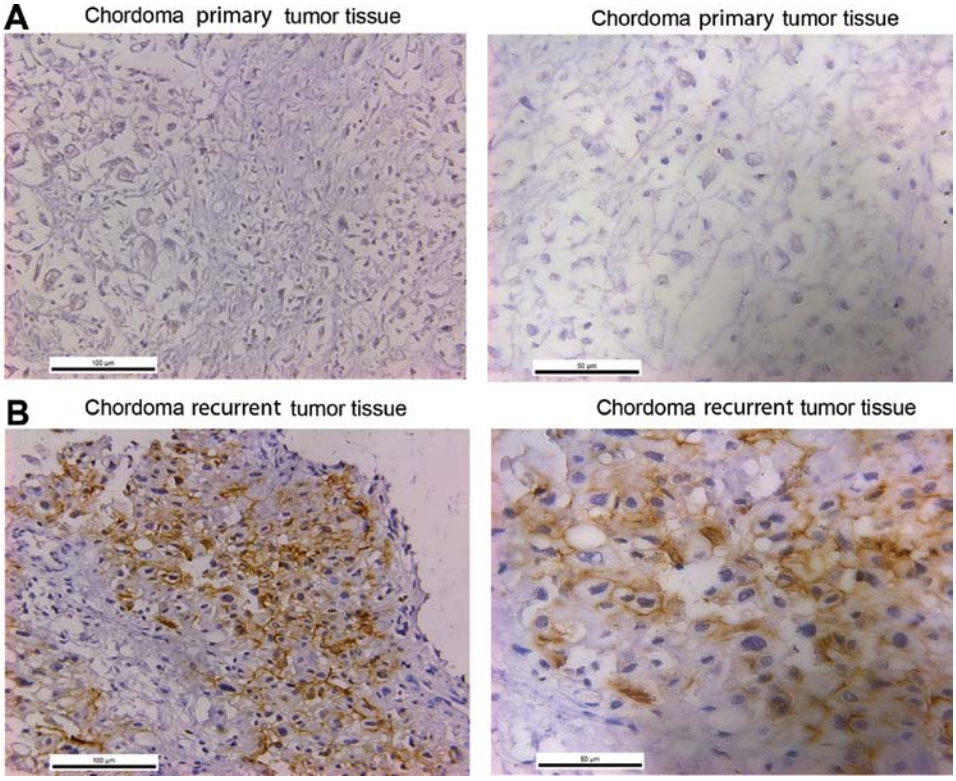

Figure 5. Immunohistochemistry of ALCAM in CSO and CSR. CSO, chordoma primary tumor; CSR, recurrent tumor.

terms. The proteins were found to be involved in either a biological process, a cellular component and/or a molecular function (Fig. 4), indicating that there were diverse cellular components and catalytic activity change in recurrent chordomas compared to the original chordoma. Furthermore, when the identified proteins in the recurrent chordoma were mapped to the corresponding metabolic pathways, many key cellular pathways including amino acid, carbohydrate metabolism, energy, and nucleotide metabolism were found to be downregulated (Fig. 4).

In order to confirm our results from the proteome, we examined tumor-related protein expression from the list of upregulated proteins through IHC in the chordoma patient primary and CSR tissues. ALCAM (or CD166) is a 100-105 kDa type I transmembrane glycoprotein that is a member of the immunoglobulin superfamily of proteins (21). ALCAM has been reported as a cancer stem cell marker for non-small cell lung cancer (NSCLC) (15). Physiologically, it plays a role in the development of different tissues during embryogenesis. It is also expressed in various malignant lesions such as melanoma and esophageal, gynecologic, prostate, and pancreatic cancers, and its expression is associated with diverse outcomes in different tumors (22-32). But the expression of ALCAM in chordomas has never been reported and the association between ALCAM and chordoma prognosis is not fully elucidated. In our study, we firstly detected ALCAM expression by using IHC in chordoma patient primary and CSR tissues. Fig. 5A clearly demonstrates that the primary chordoma tumor was negative for staining; however, the CSR had strong expression of ALCAM which suggests that ALCAM is a positive biomarker for recurrent chordomas and may play important roles for chordoma recurrence (Fig. 5B).

In conclusion, we analyzed the proteomic profile of a chordoma patient CSO and CSR and identified 359 proteins and 21 pathways with significant changes between CSO and CSR. Many of these molecular changes are reported in chordomas for the first time. Further investigation of the potential roles of these proteins in chordoma aggression is of interest. We also firstly found that the recurrent chordoma tumor showed enhanced carbohydrate metabolism, and the cancer stem cell marker ALCAM (CD166) expression level was increased markedly in CSR. The present study can serve as the basis for further research of recurrent chordomas.

Acknowledgements

The present study was supported by the National Nature Science Foundation for Distinguished Young Scholars of China (no. 81102036/H1624), the National Basic Research Program (no. 81272943), and the Nature Science Foundation of Shanghai (no. 12JC1411300).

References

1. Stacchiotti S, Casali PG, Lo Vullo S, *et al*: Chordoma of the mobile spine and sacrum: a retrospective analysis of a series of patients surgically treated at two referral centers. Ann Surg Oncol 17: 211-219, 2010.
2. DeLaney TF, Liebsch NJ, Pedlow FX, *et al*: Phase II study of high-dose photon/proton radiotherapy in the management of spine sarcomas. Int J Radiat Oncol Biol Phys 74: 732-739, 2009.
3. Zhou H, Chen CB, Lan J, *et al*: Differential proteomic profiling of chordomas and analysis of prognostic factors. J Surg Oncol 102: 720-727, 2010.
4. Wisniewski JR, Zougman A, Nagaraj N and Mann M: Universal sample preparation method for proteome analysis. Nat Methods 6: 359-362, 2009.

5. Vogel C and Marcotte EM: Calculating absolute and relative protein abundance from mass spectrometry-based protein expression data. Nat Protoc 3: 1444-1451, 2008.
6. Lu P, Vogel C, Wang R, Yao X and Marcotte EM: Absolute protein expression profiling estimates the relative contributions of transcriptional and translational regulation. Nat Biotechnol 25: 117-124, 2007.
7. Benjamini Y and Hochberg Y: Controlling the false discovery rate - a practical and powerful approach to multiple testing. J R Stat Soc B 57: 289-300, 1995.
8. Conesa A, Gotz S, Garcia-Gomez JM, Terol J, Talon M and Robles M: Blast2GO: a universal tool for annotation, visualization and analysis in functional genomics research. Bioinformatics 21: 3674-3676, 2005.
9. Yamada T, Letunic I, Okuda S, Kanehisa M and Bork P: IPath2.0: interactive pathway explorer. Nucleic Acids Res 39: W412-W415, 2011.
10. Shimizu-Hirota R, Sasamura H, Kuroda M, Kobayashi E and Saruta T: Functional characterization of podocan, a member of a new class in the small leucine-rich repeat protein family. FEBS Lett 563: 69-74, 2004.
11. Hoover KB, Liao SY and Bryant PJ: Loss of the tight junction MAGUK ZO-1 in breast cancer: relationship to glandular differentiation and loss of heterozygosity. Am J Pathol 153: 1767-1773, 1998.
12. Liu W, Liu B, Xin L, Zhang Y, Chen X, Zhu Z and Lin Y: Down-regulated expression of complement factor I: a potential suppressive protein for gastric cancer identified by serum proteome analysis. Clin Chim Acta 377: 119-126, 2007.
13. Ohnuma SI: Cancer diagnosis and treatment. Google Patents, 2011.
14. Ostrow KL, Park HL, Hoque MO, *et al*: Pharmacologic unmasking of epigenetically silenced genes in breast cancer. Clin Cancer Res 15: 1184-1191, 2009.
15. Tachezy M, Zander H and Wolters-Eisfeld G: Activated leukocyte cell adhesion molecule (CD166): an 'inert' cancer stem cell marker for non-small cell lung cancer? Stem Cells 32: 1429-1436, 2014.
16. Ibrahim SA, Reed KR, Clarke AR, Pritchard DM and Jenkins JR: Sa1992 SFRS2 and CDC5L interaction: an insight into downstream events following APC deletion during colorectal carcinogenesis. Gastroenterology 144: S353-S354, 2013.
17. Palmieri D, Bouadis A, Ronchetti R, Merino MJ and Steeg PS: Rab11a differentially modulates epidermal growth factor-induced proliferation and motility in immortal breast cells. Breast Cancer Res Treat 100: 127-137, 2006.
18. Klement RJ and Kammerer U: Is there a role for carbohydrate restriction in the treatment and prevention of cancer? Nutr Metab 8: 75, 2011.
19. Walenta S, Wetterling M, Lehrke M, Schwickert G, Sundfør K, Rofstad EK and Mueller-Klieser W: High lactate levels predict likelihood of metastases, tumor recurrence, and restricted patient survival in human cervical cancers. Cancer Res 60: 916-921, 2000.
20. Seyfried TN and Shelton LN: Cancer as a metabolic disease. Nutr Metab 7: 7, 2010.
21. Skonier JE, Bowen MA, Emswiler J, Aruffo A and Bajorath J: Recognition of diverse proteins by members of the immunoglobulin superfamily: delineation of the receptor binding site in the human CD6 ligand ALCAM. Biochemistry 35: 12287-12291, 1996.
22. Weidle HU, Eggle D, Klostermann S and Swart GW: ALCAM/CD166: cancer-related issues. Cancer Genom Proteom 7: 231-243, 2010.
23. Van Kilsdonk JW, Wilting RH, Bergers M, van Muijen GN, Schalkwijk J, van Kempen LL, and Swart GW: Attenuation of melanoma invasion by a secreted variant of activated leukocyte cell adhesion molecule. Cancer Res 68: 3671-3679, 2008.
24. Ofori-Acquah SF and King JA: Activated leukocyte cell adhesion molecule: a new paradox in cancer. Transl Res 151: 122-128, 2008.
25. Ihnen M, Müller V, Wirtz RM, *et al*: Predictive impact of activated leukocyte cell adhesion molecule (ALCAM/CD166) in breast cancer. Breast Cancer Res Treat 112: 419-427, 2008.
26. Mezzanzanica D, Fabbi M, Bagnoli M, *et al*: Subcellular localization of activated leukocyte cell adhesion molecule is a molecular predictor of survival in ovarian carcinoma patients. Clin Cancer Res 14: 1726-1733, 2008.
27. Tachezy M, Zander H, Marx AH, Stahl PR, Gebauer F, Izbicki JR and Bockhornet M: ALCAM (CD166) expression and serum levels in pancreatic cancer. PLoS One 7: e39018, 2012.
28. Tachezy M, Effenberger K, Zander H, *et al*: ALCAM (CD166) expression and serum levels are markers for poor survival of esophageal cancer patients. Int J Cancer 131: 396-405, 2012.
29. Tachezy M, Zander H, Gebauer F, Marx A, Kaifi JT, Izbicki JR and Bockhorn M: Activated leukocyte cell adhesion molecule (CD166) - its prognostic power for colorectal cancer patients. J Surg Res 177: e15-e20, 2012.
30. Tachezy M, Zander H, Marx AH, *et al*: ALCAM (CD166) expression as novel prognostic biomarker for pancreatic neuroendocrine tumor patients. J Surg Res 170: 226-232, 2011.
31. Ishiguro F, Murakami H, Mizuno T, *et al*: Membranous expression of activated leukocyte cell adhesion molecule contributes to poor prognosis and malignant phenotypes of non-small-cell lung cancer. J Surg Res 179: 24-32, 2013.
32. Simon R, Mirlacher M and Sauter G: Immunohistochemical analysis of tissue microarrays. Methods Mol Biol 664: 113-126, 2010.